Journal of Applied Polymer Science

Transparent Poly(methyl methacrylate-*co*-butyl acrylate) Nanofibers

Merih Zeynep Avcı,[1,2] A. Sezai Sarac[1]

[1]Polymer Science and Technology, Istanbul Technical University, Nanoscience and Nanoengineering, Maslak, 34469, Istanbul, Turkey

[2]Department of Chemistry, Akdeniz University, Antalya 07058, Turkey

Correspondence to: A. S. Sarac (E-mail: sarac@itu.edu.tr).

ABSTRACT: Nanofibers of *n*-Butyl Acrylate/Methyl Methacrylate copolymer [P(BA-*co*-MMA)] were produced by electrospinning in this study. P(BA-*co*-MMA) was synthesized by emulsion polymerization. The structural and thermal properties of copolymers and electrospun P(BA-*co*-MMA) nanofibers were analyzed using Fourier transform infrared spectroscopy–*Attenuated total reflectance* (FTIR–ATR), Nuclear magnetic spectroscopy (NMR), and Differential scanning calorimetry (DSC). FTIR–ATR spectra and NMR spectrum revealed that BA and MMA had effectively participated in polymerization. The morphology of the resulting nanofibers was investigated by scanning electron microscopy, indicating that the diameters of P(BA-*co*-MMA) nanofibers were strongly dependent on the polymer solution dielectric constant, and concentration of solution and flow rate. Homogeneous electrospun P(BA-*co*-MMA) fibers as small as 390 ± 30 nm were successfully produced. The dielectric properties of polymer solution strongly affected the diameter and morphology of electrospun polymer fibers. The bending instability of the electrospinning jet increased with higher dielectric constant. The charges inside the polymer jet tended to repel each other so as to stretch and reduce the diameter of the polymer fibers by the presence of high dielectric environment of the solvent. The extent to which the choice of solvent affects the nanofiber characteristics were well illustrated in the electrospinning of [P(BA-*co*-MMA)] from solvents and mixed solvents. Nanofiber mats showed relatively high hydrophobicity with intrinsic water contact angle up to 120°. © 2013 Wiley Periodicals, Inc. J. Appl. Polym. Sci. 130: 4264–4272, 2013

KEYWORDS: copolymers; nanostructured polymers; coatings

Received 23 February 2013; accepted 26 June 2013; Published online 16 July 2013

DOI: 10.1002/app.39705

INTRODUCTION

Electrospinning technique provides the production of microfibers and nanofibers from a variety of polymeric materials with porosities in the range of 30–90%, and submicrometer to 5 μm pores.[1–6] The formation of beadless uniform nano- and microfibers is possible by adjusting the polymer concentration, applied voltage, polymer molecular weight, and distance between tip and collector and injection flow rate.[7–14] The variation of the concentration of the polymer solution and molecular weight of the polymer is one of the most common ways to control the size and morphology of the electrospun fibers. When the polymer concentration is lower than a critical value, the viscosity of the solution is not high enough to maintain a stable polymer jet, so the bead formation occurs.[8,11–14] Another common way to control the diameters of the electrospun fibers is by varying the injection flow rate.[11–13] The amount of the produced polymer fibers is proportional to the flow rate, and the diameter of the polymer fibers increases as the flow rate increases.[11–13] Applied voltage and tip-collector distance are the other experimental conditions to effect on the morphology and fiber diameter of the electrospun fibers. When the applied voltage is high and the tip-collector distance is low giving strong electric field, then electrospun fibers having small diameters is obtained.[11,12,14] These nanofibers are generally used as nonwoven mats,[7] drug loaded wound dressings,[7,15] drug delivery,[7,16] tissue engineering matrices (e.g., scaffolds for bone and soft tissue regeneration),[7,17,18] catalysis, filters, membranes, sensors.[7,17]

The basic electrospinning process can be extended towards electrospinning in different solvent dielectric environment to further broaden accessible fiber architectures and potential areas of application. Since fiber morphology is affected by the dielectric constant of solvents, with solutions of high dielectric constant, the surface charge density on the jet tends to be more evenly dispersed. This provides high nanofiber quality and continuous productivity during electrospinning.[19]

Recently acrylic polymers are used for building materials sector and the protection of walls, facades, consolidation of monuments, and cultural heritage sites because of their good properties. These protective materials must be transparent, stable

against photo-oxidation, and lightweight.[20] In addition, these copolymers should also have good mechanical properties to be used for coating applications. To improve their mechanical properties various methods can be used such as electrospinning.

In this article, we reported the preparation and characterization of P(BA-*co*-MMA) nanofibers obtained by electrospinning. A series of nanofibers with various wt % of [P(BA-*co*-MMA)] in DMF, and nanofibers with various solvent mixtures with different dielectric environment were produced and characterized regarding their morphology and the chemical composition, and the resulted nanofiber mat contact angles were measured. The hydrophobicity changed by simply changing the fiber diameter, which was realized by changing the polymer solution properties during electrospinning. Such nanofibers could be used for the protection of small historical articles due to their hydrophobicity and transparency. To show the applicability for historical articles, old coins were coated by this copolymer nanofiber with a reasonable transparency (Figure 1, electrospinning details and exemplifying the transparency).

Acrylic copolymers have found great interest for the different high-performance product applications. They were used as polymer electrolytes, i.e., in Li-polymer batteries, to produce conductive composites as thin films, in addition to their very well dying properties and have excellent colorfastness.

Electrospun fibers with various diameters were achieved in this study through adjusting the solvent dielectric constant, which can be used for mentioned applications as a fiber form with controllable diameter.

In this study, it was also shown that fluorine-free hydrophobic nanofiber could be produced by a desired diameter where these fibers are a good candidate for various coating applications including technical textile fabric coatings.

EXPERIMENTAL

Materials

Methyl methacrylate (MMA), butyl acrylate (BA), polymethyl methacrylate (PMMA), dimethylformamide (DMF), tetrahydrofuran (THF), sodium dodecyl sulfate (SDS), and potassium peroxydisulfate (KPS) were purchased from Sigma Aldrich. Acetone [$(CH_3)_2CO$] and ethyl alcohol [(C_2H_5OH)] were obtained from Merck and all of them were in analytical grade.

Synthesis of P(BA-co-MMA)

Emulsifier sodium dodecyl sulfate (SDS) of 0.5 g was dissolved in 80 mL water and 50 g of a mixture of monomers of MMA and BA (25:25 wt. MMA:BA) was subsequently dropped into the reactor, and the mixture was stirred for 30 min. At the same time, 0.25 g KPS was dissolved in 20 mL pure water. After the 30 min, KPS solution was added to the mixture.[21] Reaction continued for 3 h at 80°C. After 3 h, reaction was stopped with addition of 300 mL ethanol. Finally, the mixture was washed with ethanol and water, and copolymer was dried at 50°C for 24 h in vacuum drying-oven. Copolymer conversion was found to be 65% for the 50/50% (mole) BuA/MMA feed ratio.

Preparation of Electrospinning Solutions

Five series of polymer solution with different concentration of P(BA-*co*-MMA) was dissolved in DMF, which are 1%(w/v), 3%(w/v), 5%(w/v), 8%(w/v), and 10%(w/v) P(BA-*co*-MMA). To investigate the effect of different solvents, the electrospinning solutions of 5% (w/v) P(BA-*co*-MMA) were prepared in various mixtures of solvents as well. Each solutions were stirred at room temperature with the speed of 400 rpm for 3 h. Then they were filtered to remove impurities from the solutions. The solutions were then loaded into a 2.5 mL syringe. Electrospun fibers were characterized by FTIR-ATR, DSC, and SEM measurements.

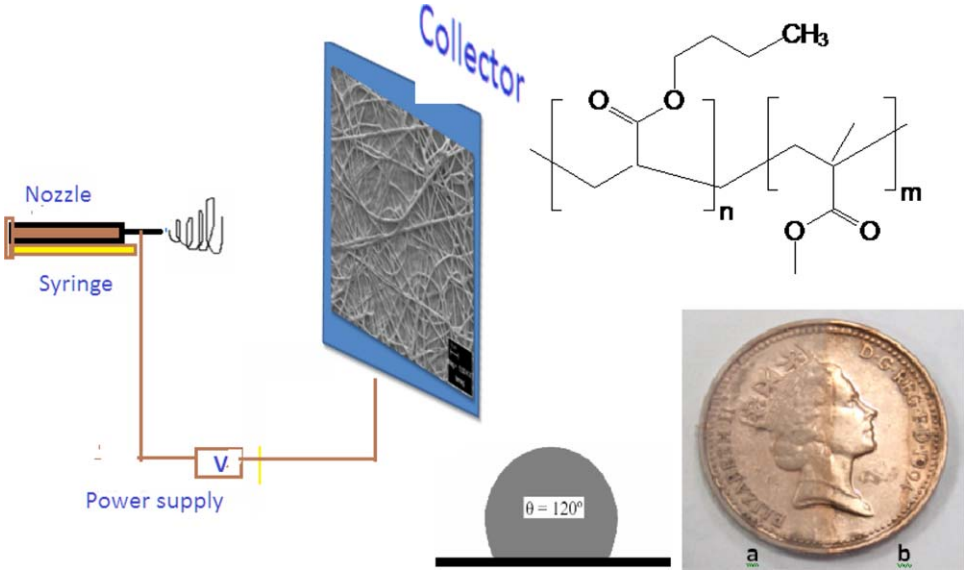

Figure 1. Electrospinning details and examplifying the transparency (a) Coated coin and (b) noncoated coin. [Color figure can be viewed in the online issue, which is available at wileyonlinelibrary.com.]

Applied Polymer SCIENCE

Process Setup and Electrospinning

In electrospinning process, the setup consisted of a DC high voltage power supply from GAMMA High Voltage Research (Model no: ES50, FL, USA) with an electrical potential constant at 15 kV, and a syringe pump (New Era Pump Systems, Model no: NE-500, NY, USA). The metal collector was covered with an aluminum foil. The setup was kept in a Plexiglas box for experimenter's safety and to have dust free medium. All experiments were carried out under atmospheric pressure and at room temperature. The positive electrode wire was hooked at the metal part of the needle and negative part of the electrode was attached to the metal collector. Operation time was sufficient for the deposition of fibers on the aluminum foil. A horizontal setup was chosen for the electrospinning process (Figure 1).

Characterization of P(BA-co-MMA) Copolymers

- FTIR spectrophotometric analysis of P(BA-*co*-MMA) nanofibers were carried out with FTIR-ATR reflectance spectrophotometer (Perkin Elmer, Spectrum One, with a Universal ATR attachment with a diamond and ZnSe crystal).
- 250 MHz Brucker AC Aspect 3000 ^{1}H NMR spectrometer was used, $CDCl_3$ as a solvent. Values were recorded as ppm relative to internal standard (TMS).
- Number average (M_n) and weight average (M_w) molecular weights were determined in ultra-pure THF solvent using GPC (Agilent 1200 series, BIC RID detector) equipment. The calibration was done by using the different molecular weight of PS standards ($M_w = 2000$ to 800,000), and the passage time of the solvent was 0.3 mL/min.
- The DSC measurements were carried out on TA Q1000 DSC instrument calibrated with PMMA. DSC measurement of polymers was operated with 4 cycles. First cycle was heated from −30°C to 150°C, second cycle was cooled from 150°C to −30°C, third cycle was heated from −30°C to 250°C and fourth cycle was cooled from +250°C to −30°C. Third cycle was considered for DSC analysis. Each sample was scanned at a heating rate of 10°C min^{-1}.
- Resulting fibers were also characterized morphologically by scanning electron microscope (two different SEM devices were used, firstly Philips XL30 and subsequently, LEO SUPRA 35 VP) and the samples for the SEM measurements were prepared by coating of gold (Ion Sputter Metal Coating Device, MCM-100).
- Contact angles on electrospun fiber layer surfaces under air were measured by using a KSV-CAM 100 contact angle meter with a PC controlled motorized syringe within ±1° precision. Water liquid drop used was spectroscopic grade.
- Nanofiber films have shown transparency throughout the entire visible region until 400 nm, blocking UV light.

RESULTS AND DISCUSSION

FTIR–ATR Spectrophotometric Analysis of P(BA-co-MMA)

The FTIR–ATR spectra of PMMA and [P(BA-*co*-MMA)] of polymer granules and [P(BA-*co*-MMA)] nanofibers were shown in Figure 2 and they were recorded in the absorbance mode. Figure 2 shows the peaks at 2950, 1728, 1435, and 1149 cm^{-1} assigned to CH stretching, C═O stretching, CH_3 stretching and

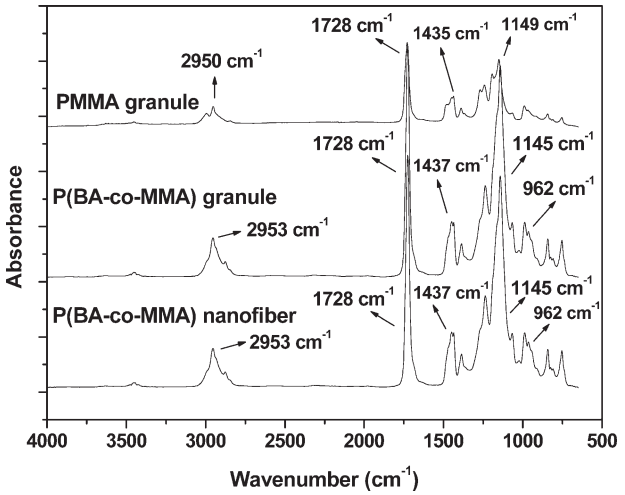

Figure 2. FTIR–ATR spectrums of PMMA granules, P(BA-*co*-MMA) granules and P(BA-*co*-MMA) nanofibers.

O—CH_3 stretching vibrations, in PMMA. Poly(butylacrylate) (PBA) and PMMA had similar molecular backbones, only slight differences were found in their FTIR spectra. Absorption at 962 cm^{-1}, which is the stretching vibration of C(sp(2))-H of BA in [P(BA-*co*-MMA)] in agreement with the Ref. 22.

Nuclear Magnetic Resonance Measurements (NMR) of P(BA-*co*-MMA)

Figure 3 shows the ^{1}H-NMR spectra of copolymers recorded in $CDCl_3$ using TMS as the internal standard. The peak at $\delta = 3.99$ ppm was due to the —OCH_2 groups of PBA and the peak at $\delta = 3.64$ ppm was due to —OCH_3 group of PMMA. [other peaks $\delta = 2.03$ ppm (α—CH), $\delta = 1.38$ ppm (—$^2CH_2$—), $\delta = 1.57$ ppm(—$^3CH_2$)— and $\delta = 0.91$ ppm (—$^4CH_3$ of *n*-butyl acrylate) and $\delta = 1.08$ ppm and $\delta = 1.22$ ppm (α-CH_3 of MMA), and $\delta = 7.24$ ppm was due to $CDCl_3$. Moreover, another peak was observed at $\delta = 3.46$ due to remaining ethanol in the copolymer structure used for precipitation.

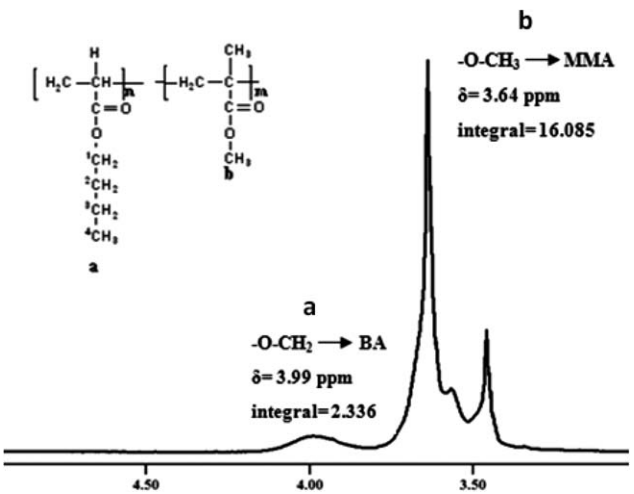

Figure 3. NMR spectrum of P(BA-*co*-MMA).

The qualitative amount of functional groups of MMA and BA in the copolymers was estimated from the integral ratio of methyl protons (—$COOCH_3$) and methylene protons (—$COOCH_2$) by integration of each peak in standard way.[23,24] The mole fraction of MMA in the copolymer (F_{MMA}) calculated as 0.80; and F_{BA} calculated as 0.18.[25] According to the literature, MMA has a higher reactivity ratio,[26–30] so it tends to react with itself more than BA during polymerization. Thus, the mole fraction of MMA was found to be higher than that of BA.

Differential Scanning Calorimetry Measurement (DSC) of P(BA-co-MMA)

Glass transition temperature (T_g) values of the PMMA and [P(BA-*co*-MMA)] were determined as 117.9°C and 48.5°C (Figure 4 shows the T_g values of the [P(BA-*co*-MMA)] for exo up), and it was realized that the presence of the BA content in the copolymers caused a decrease in the T_g values due to the increase in the number of —CH_2— group in the copolymer. Increasing the number of this unit caused increase in the main chain flexibility. Therefore, T_g value of copolymer obtained was lower than that of PMMA.[31]

In the literature, T_g value of PMMA homopolymer was reported as 105°C,[32] T_g value of PBA was between (−)49°C and (−)54°C[33,34] and T_g value of P(BA-*co*-MMA) copolymer was reported as 41.8°C[35] and 53°C.[36] Increasing BA content in the BA/MMA copolymer structure caused a decrease in T_g value due to the increasing main chain flexibility.[37]

In this study, T_g value of P(BA-*co*-MMA) was found to be higher than the literature value. The reason for this could be attributed to the higher reactivity of MMA.[27–30,37] This difference in reactivity led to longer sequences of MMA, resulting the T_g of the copolymer higher than expected.[26]

Molecular Weight Determination

M_n and M_w values were obtained from GPC (M_w (kg/mol): 663, M_n (kg/mol): 518), Polydispersity index (PDI) of copolymers, which were calculated from M_w/M_n (PDI: 1.29) and the copolymer intrinsic viscosities (η) in chloroform solutions were determined by using an Ubbelohde-type viscometer (η (dL/g): 178).

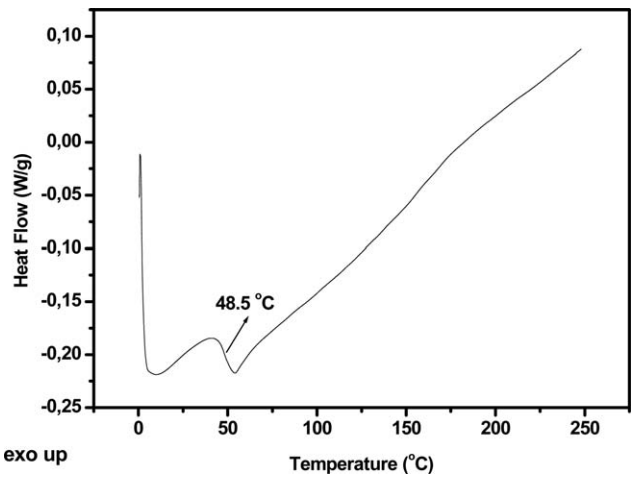

Figure 4. DSC graph of P(BA-*co*-MMA).

Morphology of Fibers

Effect of Concentration of Solution on Nanofiber Diameters. Five different samples were prepared by varying the concentration of P(BA-*co*-MMA) in DMF: 1, 3, 5, 8, and 10 wt % of P(BA-*co*-MMA) in DMF and effect of concentration on the diameters of nanofibers was examined. Therefore, electrospinning parameters were kept the same for all solutions (Figure 5).

Figure 6 shows the scanning electron microscopy (SEM) images of P(BA-*co*-MMA) nanofibers electrospun from 3, 5, 8, and 10 wt % P(BA-*co*-MMA) solution in DMF. The average diameters of electrospun fibers at different concentrations were determined by using Adobe Acrobat 8 Professional to randomly measure the diameters of 50 individual fibers shown in SEM images with 5000× magnitude. The diameters of the fibers increased slightly as the concentration of the P(BA-*co*-MMA) solution was increased (Figure 5). An increase in the concentration resulted in greater polymer chain entanglements within the solution, which was necessary to maintain the continuity of the jet during electrospinning. We found that the P(BA-*co*-MMA) solutions yielded bead-free nanofibers due to the greater polymer chain entanglements and viscosity of the solutions, but fiber forms were not observed. For 1% (w/v) P(BA-*co*-MMA) solution due to the smaller polymer chain entanglements, and surface tension effects could be dominant with decreased polymer concentration/solution viscosity. So, the concentration of P(BA-*co*-MMA) solution was increased to 3% (w/v) and uniform bead-free P(BA-*co*-MMA) nanofibers were obtained with a diameter of 390 ± 30 nm. This revealed that a high concentration/viscosity was required to produce uniform bead-free P(BA-*co*-MMA) nanofibers, but especially the 5 wt % [P(BA-*co*-MMA)] solution seems to be the best electrospinning solution under these conditions due to continous and homogeneous fiber production.

Effect of Dielectric Constant of Solvent (Mixture) on Nanofiber. To determine an optimum solvent system for electrospinning of P(BA-*co*-MMA), different solvents and solvent mixtures were studied. Three solvents with different dielectric constants

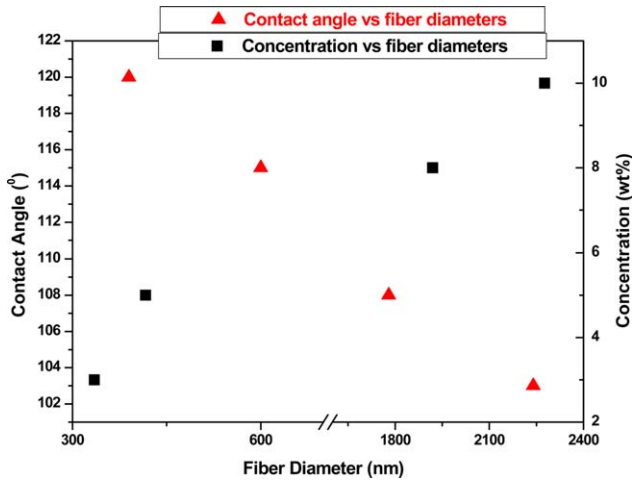

Figure 5. Contact angle and concentration versus fiber diameters. [Color figure can be viewed in the online issue, which is available at wileyonlinelibrary.com.]

Applied Polymer SCIENCE

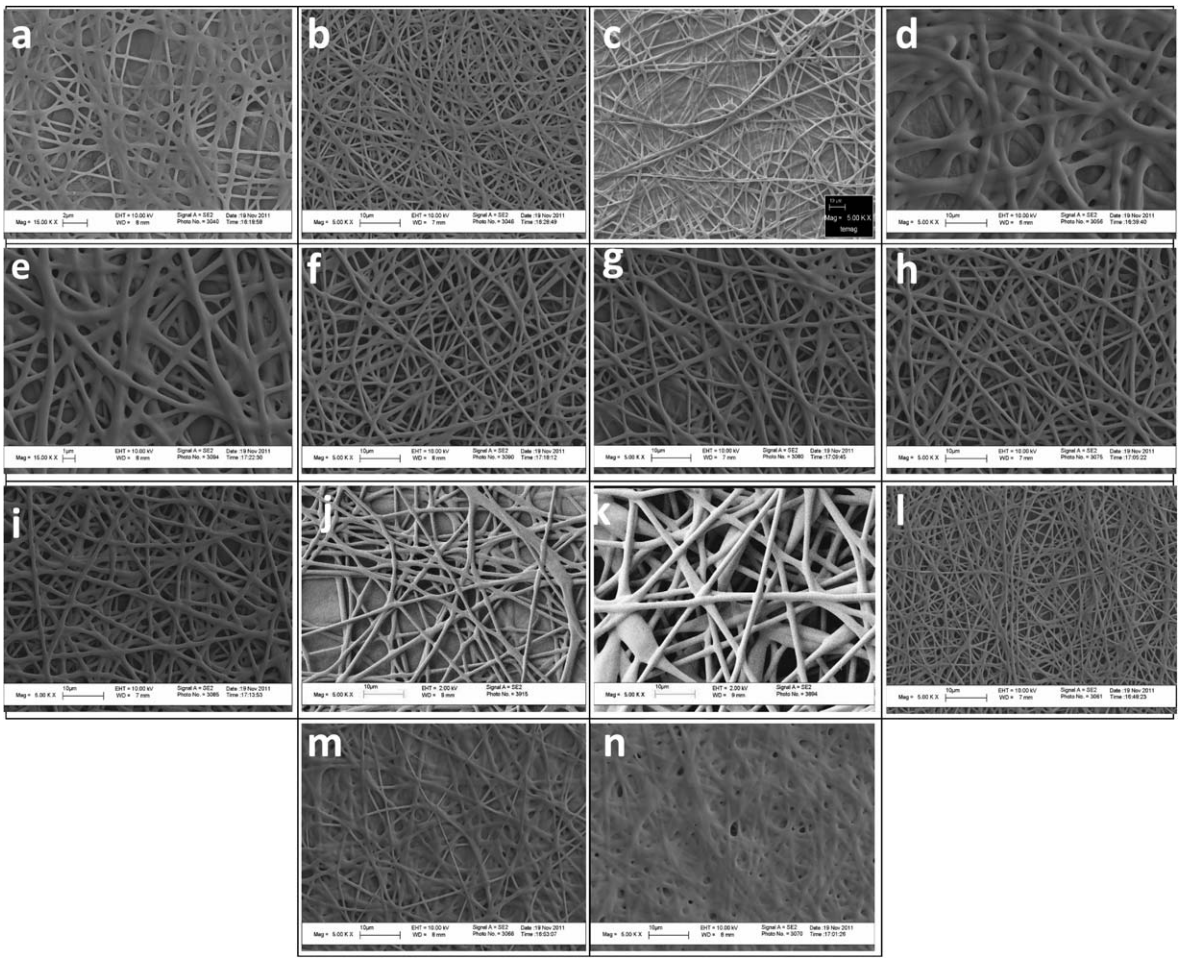

Figure 6. SEM images of the electrospun fibers at different P(BA-*co*-MMA)/DMF concentrations: (a) 3 wt % (390 ± 30 nm), (b) 5 wt % (600 ± 50 nm), (c) 8 wt % (1780 ± 100 nm), and (d) 10 wt % (2240 ± 40 nm) and at different solvent-solvent mixtures (e) 5 wt % DMF/THF(75/25), (f) 5 wt % DMF/Acetone, (g) 5 wt % DMF/THF(50/50), (h) 5 wt % acetone, (i) 5 wt % DMF/THF(25/75), (j) 5 wt % THF/acetone, (k) 5 wt % THF (all electrospinning conditions were the same for all samples Flow rate: 1 mL/h, Distance: 15 cm, Applying Voltage: 15 kV) and at different flow rates (l) 3 mL/h (820 ± 10 nm), (m) 5 mL/h (990 ± 50 nm), (n) 7 mL/h (1180 ± 80 nm). (Another electrospinning conditions were the same for all samples. Distance: 15 cm, Applying voltage: 15 kV).

were used to prepare P(BA-*co*-MMA) solution at a fixed polymer concentration of 5 wt %. Dielectric constant (ε_m) of the solvent mixture was calculated by the following equation:

$$\varepsilon_m = \varepsilon_1 x_1 + \varepsilon_2 x_2 \quad (1)$$

where ε_1 was the dielectric constant of the solvent 1 and x_1 was the corresponding volume fraction.[38] The dielectric constant ε of a material was essentially a measure of how effectively it concentrates the electrostatic lines of flux when placed in an electric field. In a practical sense, it was a measure of how much electrical charge the solvent was capable of holding. Solvents with different values of ε used in electrospinning interact very differently with the electrostatic field, and it was therefore an important material parameter in electrospinning.[19] With solutions of high dielectric constant, the surface charge density on the jet tended to be more evenly dispersed. This provided high nanofiber quality and productivity during electrospinning.[19] The effect of solvent dielectric on fiber morphology was illustrated by the comparison of the quality of nanofibers, and when the solutions had high ε, the electrospinning yields nanofibers that had the smaller average diameters (nm).[39–45]

The extent to which the choice of solvent affects the nanofiber characteristics were well illustrated in the electrospinning of [P(BA-co-MMA)] from solvents and mixed solvents. As the volume fraction of DMF in the mixture was increased from 25 to 100 v/v, the average diameter (nm) (at the same polymer concentration; 5 wt %) decreased from 1600 ± 80 nm to 600 ± 20 nm (Table I). This was a result of the increased dielectric constant of the solution due to addition of DMF [ε(DMF); 36.7, ε(Acetone); 20.7 and ε(THF); 7.47].

Under the same flow rate (1 mL/h), applied voltage (15 kV) and spinning distance (15 cm), a solution with a higher electrical conductivity could cause higher elongation of a jet along its axis and electrospinning fibers with smaller diameter.

Figure 6 also shows the SEM images of P(BA-*co*-MMA) nanofibers electrospun from 5% (w/v) P(BA-*co*-MMA) solution in different solvents (DMF, acetone, and THF). Bead-free nanofibers

Table I. Dielectric Constants of Different Solvents and Diameter of Resulting Nanofibers Prepared in These Solvents[a,b]

Exp. code	Solvents	Mixture ratio of solvents (v/v)	Dielectric constant	Diameter of nanofibers (nm)
6b	DMF	100	36.71[a]	600 ± 20
6e	DMF/THF	75/25	29.40[b]	680 ± 40
6f	DMF/Acetone	50/50	28.705[b]	720 ± 25
6g	DMF/THF	50/50	22.09[b]	800 ± 30
6h	Acetone	100	20.7[a]	870 ± 40
6i	DMF/THF	25/75	14.78[b]	995 ± 50
6j	THF/Acetone	50/50	14.085[b]	1200 ± 40
6k	THF	100	7.47[a]	1600 ± 80, beaded fibers

Electrospinning conditions and polymer solution concentrations were the same for all samples. Flow rate: 1 mL/h, Distance: 15 cm, Applying voltage: 15 kV and 5 wt %.
[a] Dielectric constants were obtained from the literature.
[b] Dielectric constants of solvent mixture were obtained from the eq. (1).

were obtained for the polymer solutions having high dielectric constant. Figure 6(b) shows the nanofibers of 5% DMF solution. It had the lowest diameters of nanofibers among the others due to its highest dielectric constant, where highest dielectric constant provided high nanofiber quality and productivity during electrospinning.[19]

The dielectric properties of solutions strongly affected the diameter and morphology of electrospun polymer fibers. The bending instability of the electrospinning jet also increased with higher dielectric constant, by facilitating the reduction of the fiber diameter due to the increased jet path.[41]

SEM images of the electrospun fibers at different P(BA-*co*-MMA)/DMF at different polymer concentrations [given in Figure 6(a–c)] have shown similar homogenity except higher diameters [Figure 6(d)].

As the solution viscosity increases, molecular entanglement increases as fibers can translates from uniform fibers to flat fibers [Figure 6(d)].

Flat fibers are also observed at different solvent–solvent mixtures DMF/THF(75/25) [Figure 6 (e)] and for feed rate of solution 5 and 7 mL/h [Figure 6(m,n)] due to the high polymer content in last two cases.

Table I indicates the effect of solvent mixture ratio on dielectric constant and fiber diameter by using DMF/THF solution mixture. Since DMF had lower vapor pressure and THF had higher, it was expected to evaporate slowly after deposition of fibers on the target for DMF case. Therefore, at lower DMF/THF (25/75) ratios, rate of the solvent evaporation from the fiber surface increased due to the large volume of THF in the polymer solution and caused the fiber diameters increase [Figure 6(i,g,e)]. During the electrospinning of P(BA-*co*-MMA) with increased THF ratios in DMF/THF mixture, the solution was noticed to loose the capability to form more fibers than the beaded ones due to higher THF evaporation rate. It was expected that surface tension of DMF/THF (25/75) gradually increased, and thus, the solution lost the capability to form more fibers against the relatively higher surface tension. As a result, increasing THF content in the mixture caused fiber diameter increase [Figure 6(k)].

Significant changes in fiber diameter and morphology with various processing parameters including solvent vapor pressure and dielectric constant were realized, i.e., different fiber diameters were observed. Moreover, the solution jet evaporated or solidified, and was collected as an interconnected web of small fibers. Figure 7 shows relationship between dielectric constant and diameter of nanofibers.

The charge density around the nanofiber by the solvent depended on the solution's electrical properties (i.e., its electric conductivity related to the amount of dissolved electrolyte admixture and ion mobility, and dielectric constant of the solvent) and applied electric potential. The experimental data on the effect of solvent dielectric constant, at constant applied voltage, and nozzle-to-collector distance on the electric current i.e., volumetric charge densities effect was observed during electrospinning.[46] These results led to a conclusion that volumetric charge density depended on each of these parameters through a power-law relationship, except that the volumetric charge density depended on the nozzle-to-collector distance through an exponential relationship. These charged ions (polymer and its solvation atmosphere by solvent) moved in response to the applied electric field towards the electrode of opposite polarity, thereby transferring tensile forces to the polymer liquid.

In electrospinning technique, the ejected charged jet was affected by electrical forces, so it needed to have high electrical properties such as good dielectric constant to enhance the density of charges at the surface of jet for better stretching and uniform formation of fibers with bead-free morphology.

The copolymer with hydrogen bonding groups displayed an increase in intermolecular associations with decreasing solvent dielectric constant.

Moreover, strong intermolecular associations between the functional groups were readily observed in the nonpolar solvents with the production of significantly larger electrospun fibers due to an increased effective molecular weight of the polymer

Applied Polymer SCIENCE

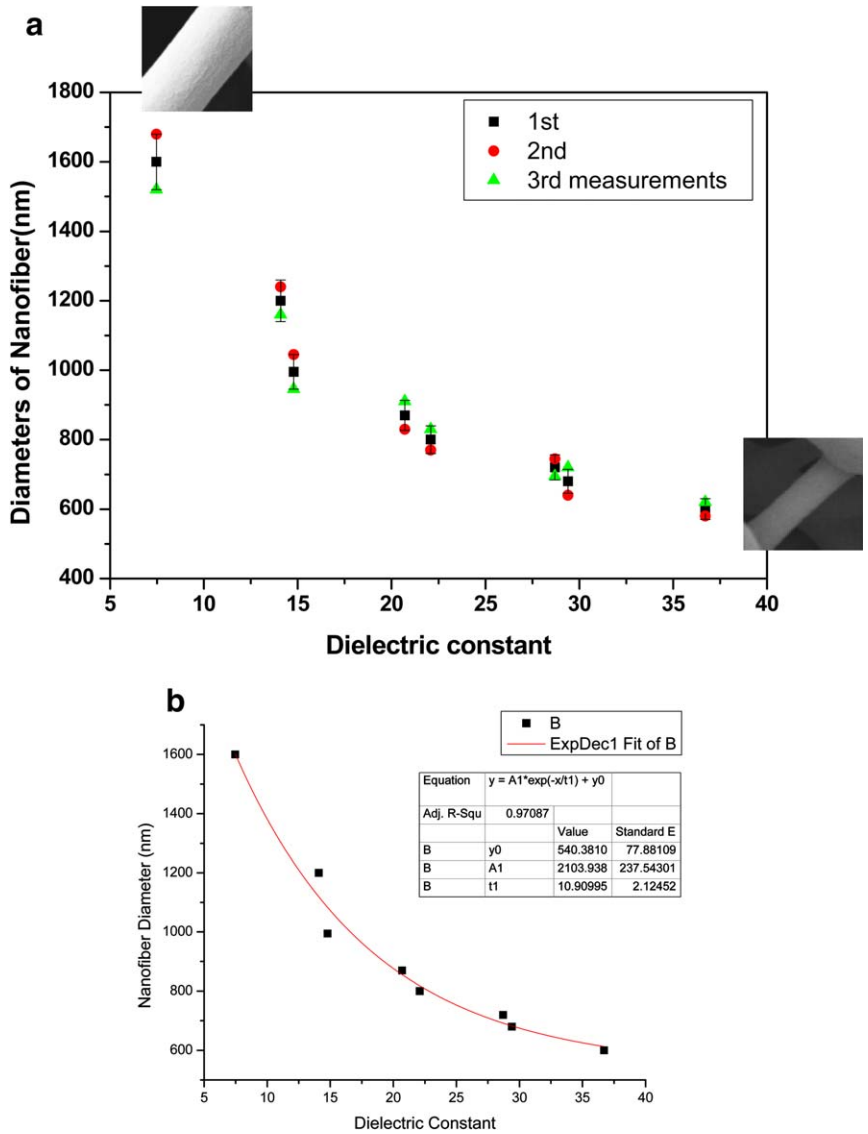

Figure 7. (a) Relationship between average diameter (average of three experiments) of resulting nanofibers and dielectric constant of solvents and solvent mixtures. (The average diameter of electrospun fibers were determined by using Adobe Acrobat 8 Professional to randomly measure the diameters of 50 individual fibers shown in SEM images with 5000× magnitude) and (b) the equation fitting well with the experimental data. [Color figure can be viewed in the online issue, which is available at wileyonlinelibrary.com.]

chains. The following equation fitted best to the experimental data obtained in this study by nonlinear regression between the average nanofiber diameter denoted as ***r***, and dielectric constant of solvent or solvent mixture denoted as ε. Figure 7 shows how experimental and calculated values well-fitted according to this equation.

$$r = 540 + 2100e^{-0.1\varepsilon}$$

Our results led to a conclusion that average diameter of nanofibers (r) depended on dielectric constant (ε) of solvent or solvent mixture through an exponential relationship given above under this study conditions by holding other parameters constant.

Effect of Flow Rate on Nanofiber. Flow rate on morphology of electrospun fibers was studied using DMF as a solvent in the presence of 5 wt % P(BA-*co*-MMA). When the flow rate increased, a corresponding increase in the fiber diameter was observed (Figure 6). The diameters of [P(BA-*co*-MMA)] fibers ranged from 390 to 1180 nm and the morphology of the electrospun [P(BA-*co*-MMA)] fibers was not significantly changed except for Figure 6(n). Increasing flow rate provided a greater volume of solution, polymer solution was drawn away from the needle tip, jet took a long time to dry.[47] Thus, solvent had not enough time to evaporate, this situation caused fibers to fuse together such as in Figure 6(n).

Contact Angle Measurement

Equilibrium (θ_e) contact angle measurement results for water droplets on electrospun fiber surfaces (3, 5, 8, 10 wt % in DMF) were given in Figure 5. These results indicated that, the electrospun copolymeric nanofibers were hydrophobic with a

water contact angle changed from 103° to 120° depending on fiber size.

Figure 5 indicated that diameters of nanofiber had an effect on the contact angle (increase from 103° to 120°) and corresponding nanofiber diameter (from 390 to 2240 nm) where minimum contact angle was obtained in the case of maximum nanofiber diameter. According to the Xiang et al. and Asmatulu et al. results, smaller fibers had higher contact angle than that of larger fibers for the same samples.[48–50] Accordingly, in this study, 10 wt % P(BA-*co*-MMA) exhibited the highest diameter by having the lowest contact angle where increasing fiber diameter led to decrease in contact angle.

The reason for this is because drops are in contact with the solid polymer fibers and air is present in the pore spaces between the fibers. The net effect is that the drop does not experience the same forces as it normally would compare to the surface of a smooth continuous solid surface. On the porous fiber membrane, the droplet can have a contact angle 120° showing hydrophobic properties.

CONCLUSION

Electrospun fibers with various diameters were achieved through adjusting the solvent dielectric constant. SEM images indicated that the diameters of [P(BA-*co*-MMA)] nanofibers were strongly dependent on polymer solution concentrations, dielectric constant, and flow rate of solution. The diameter of electrospun [P(BA-*co*-MMA)] fibers ranged from 390 to 1180 nm under our experimental conditions.

The diameters of the fibers increased slightly as the concentration of the P(BA-*co*-MMA) solution were increased, and bead-free nanofibers and smaller fibers were obtained for the polymer solutions having high dielectric constant. As the flow rate increased, fiber diameter increased due to a greater volume of solution fiber was drawn away from the needle tip. An experimental equation was derived between average nanofiber diameter versus dielectric constant of solvent or solvent mixture for the present experimental conditions, and the electrospun copolymeric nanofibers exhibited high hydrophobic behavior with intrinsic water contact angle varied from 103° to 120° depending on the fiber size.

REFERENCES

1. Yano, T.; Yah, W. O.; Yamaguchi, H.; Terayama, Y.; Nishihara, M.; Kobayashi, M.; Takahara, A. *Chem. Lett.* **2010**, *39*, 1110.
2. Ma, M.; Mao, Y.; Gupta, M.; Gleason, K. K.; Rutledge, G. G. *Macromolecules* **2005**, *38*, 9742.
3. Tuteja, A.; Choi, W.; Ma, M. L.; Mabry, J. M.; Mazzella, S. A.; Rutledge, G. C.; McKinley, G. H.; Cohen, R. E. *Science* **2007**, *318*, 1618.
4. Tuteja, A.; Choi, W.; Mabry, J. M.; McKinley, G. H.; Cohen, R. E. *Proc. Natl. Acad. Sci. U S A* **2008**, *105*, 18200.
5. Acatay, K.; Simsek, E.; Yang, C. O.; Menceloglu, Y. Z. *Angew. Chem. Int. Ed.* **2004**, *43*, 5210.
6. Wu, W.; Zhu, Q.; Qing, F.; Han, C. C. *Langmuir* **2009**, *25*, 17.
7. Huang, Z. M.; Zhang, Y. Z.; Kotaki, M.; Ramakrishna, S. *Compos. Sci. Technol.* **2003**, *63*, 2223.
8. Nakashima, R.; Watanabe, K.; Lee, Y.; Kim, B. S.; Kim, I. S. *Adv. Polym. Tech.* **2013**, *32*, E44.
9. Greiner, A.; Wendorff, J. H. *Angew. Chem. Int. Ed.* **2007**, *46*, 5670.
10. Fong, H.; Chun, I.; Reneker, D. H. *Polymer* **1999**, *40*, 4585.
11. Yuan, X.; Zhang, Y.; Dong, C.; Sheng, J. *Polym. Int.* **2004**, *53*, 1704.
12. Chen, J. T.; Chen, W.L.; Fan, P.W. *ACS Macro. Lett.* **2011**, *1*, 41.
13. Koski, A.; Yim, K.; Shivkumar, S. *Mater. Lett.* **2004**, *58*, 493.
14. Wang, C.; Hsu, C. H.; Lin, J. H. *Macromolecules* **2006**, *39*, 7662.
15. Khil, M. S.; Cha, D. I.; Kim, H. Y.; Kim, I. S.; Bhattarai, N. *J. Biomed. Mater. Res. B* **2003**, *67B*, 675.
16. Zeng, J.; Xu, X.; Chen, X.; Liang, Q.; Bian, X.; Yang, L.; Jing, X. *J Controlled Release* **2003**, *92*, 3.
17. Fang, J.; Niu, H.; Lin, T.; Wang, X. *Chin. Sci. Bull.* **2008**, *53*, 2265.
18. Yoshimoto, H.; Shin, M.; Terai, H. *Vacant J. Biomater.* **2003**, *24*, 2077.
19. Wannatong, L.; Sirivat, A.; Supaphol, P. *Polym. Int.* **2004**, 53, **1851**.
20. Ramos-Fernández, J. M.; Guillem, C.; Lopez-Buendía, A.; Paulis, M.; Asua, J. M. *Prog. Organic Coat.* **2011**, *72*, 438.
21. Yuan, X.; Huo, D.; Qian, Q. *J. Colloid Interface Sci.* **2010**, *346*, 72.
22. Ramesh, S.; Leen, K. H.; Kumutha, K.; Arof, A. K. *Spectrochim. Acta Part A* **2007**, *66*, 1237.
23. Xie, H. Q.; Liu, X. H.; Guo, J. S. *J. Appl. Polym. Sci.* **2003**, *89*, 2982.
24. Taweerat, T.; Phattanarudee, S. *Macromol. Symp.* **2010**, *296*, 583.
25. Manders, B. G.; Smulders, W.; Aerdts, A. M.; Herk, V. *Macromolecules* **1997**, *30*, 322.
26. Kim, Y. S.; Wright, J. B.; Grunlan, J. C. *Polymer* **2008**, *49*, 570.
27. Hua, H.; Dube, M. A. *Polymer* **2001**, *42*, 6009.
28. Aerdts, A. M.; German, A. L. *Magn. Reson. Chem.* **1994**, *32*, 72.
29. Chiefari, J.; Jeffery, J.; Julia Krstina, J.; Moad, C.L.; Moad, M.; Postma, A.; Rizzardo, E.; Thang, S. H. *Macromolecules* **2005**, *38*, 9037.
30. Buback, M.; Feldermann, A.; Barner-Kowollik, C. *Macromolecules* **2001**, *34*, 5439.
31. Roy, P.; Jana, A. M.; Das, D.; Nath, D. N. *Chem. Phys. Lett.* **2009**, *474*, 297.
32. Park, I. J.; Lee, S. B.; Choi, C. K. *Polymer* **1997**, *38*, 2523.

33. http://www.dow.com/products/product_detail.page?product=1010166&application=1120093.
34. http://www.polymerprocessing.com/polymers/PBA.html.
35. Liu, Y.; Haley, J. C.; Deng, K.; Lau, W.; Winnik, M. A. *Macromolecules* **2007**, *40*, 6422.
36. Yu, H.; Peng, J.; Zhai, M.; Li, J.; Wei, G.; Qiao, J. *Radiat. Phys. Chem.* **2007**, *76*, 1746.
37. Grunlan, J. C.; Ma, Y.; Grunlan, M. A.; Gerberich, W. W.; Francis, L. F. *Polymer* **2001**, *42*, 6913.
38. Tan, S. H.; Inai, R.; Kotaki, M.; Ramakrishna, S. *Polymer* **2005**, *46*, 6128.
39. Min, B. M.; You, Y.; Kim, J. M.; Lee, S. J.; Park, W. H. *Carbohydr. Polym.* **2004**, *57*, 285.
40. Son, W. K.; Youk, J. H.; Lee, T. S.; Park, W. H. *Polymer* **2004**, *45*, 2959.
41. Hsu, C. M.; Shivkumar, S. *Macromol. Mater. Eng.* **2004**, *289*, 334.
42. Lee, K. H.; Kim, H. Y.; Khil, M S.; Ra, Y. M.; Lee, D. R. *Polymer* **2003**, *44*, 1287.
43. Dong, H.; Nyame, V.; MacDiarmid, A. G.; Jones, W. E. Jr. *J. Polym. Sci. Part B: Polym. Phys.* **2004**, *42*, 3934.
44. You, Y.; Lee, S. J.; Min, B.-M.; Park, W. H. *J. Appl. Polym. Sci.* **2006**, *99*, 1214.
45. Lee, K. H.; Kim, H. Y.; La, Y. M.; Lee, D. R.; Sung, N. H. *J. Polym. Sci. Part B: Polym. Phys.* **2002**, *40*, 2258.
46. Thompson, C. J.; Chase, G. G.; Yarin, A. L.; Reneker, D. H. *Polymer* **2007**, *48*, 6913.
47. Zong, X. H.; Kim, K.; Fang, D.; Ran, S. F.; Hsiao, B. S.; Chu, B. *Polymer* **2002**, *43*, 16.
48. Asmatulu, R.; Ceylan, M.; Nuraje, N. *Langmuir* **2011**, *27*, 504.
49. Choi, G. R.; Park, J.; Ha, J. W.; Kim, W.-D.; Lim, H. *Macromol. Mater. Eng.***2010**, *295*, 995.
50. Han, D.; Steckl, A. *J. Langmuir* **2009**, *25*, 9454.